

# Discovery of a Low-Mass Brown Dwarf Companion of the Young Nearby Star G 196-3

Rafael Rebolo,\* María R. Zapatero Osorio, Santiago Madruga, Víctor J. S. Béjar, Santiago Arribas, Javier Licandro

A substellar-mass object in orbit at about 300 astronomical units from the young low-mass star G 196-3 was detected by direct imaging. Optical and infrared photometry and low- and intermediate-resolution spectroscopy of the faint companion, hereafter referred to as G 196-3B, confirm its cool atmosphere and allow its mass to be estimated at  $25^{+15}_{-10}$  Jupiter masses. The separation between the objects and their mass ratio suggest the fragmentation of a collapsing cloud as the most likely origin for G 196-3B, but alternatively it could have originated from a protoplanetary disc that has been dissipated. Whatever the formation process was, the young age of the primary star (about 100 million years) demonstrates that substellar companions can form on short time scales.

Direct imaging searches for brown dwarfs and giant planets around stars explore a range of physical separations complementary to that of radial velocity measurements and provide key information on how substellar-mass companions are formed. Any companion uncovered by an imaging technique can be further investigated by spectroscopy, which allows information about its atmospheric conditions and evolutionary status to be obtained. So far, only one unambiguous brown dwarf companion to a star has been imaged (1) and subsequently investigated in detail (2–4). Young, nearby, cool dwarf stars are ideal targets of searches for substellar-mass companions (brown dwarfs and giant planets) using direct imaging techniques, because (i) young substellar objects are considerably more luminous when undergoing the initial phases of gravitational contraction (5–7) than at later stages; (ii) stars in the solar neighborhood (that is, within 50 pc of the sun) allow the detection of faint companions at physical separations of several tens of astronomical units; and (iii) cool stars are among the least luminous stars, which favors full optimization of the dynamic range of current detectors to achieve detection of extremely faint companions by means of narrow-band imaging techniques at red wavelengths.

Using x-ray emission as an indicator of youth (8–10), we have selected a number of late-type stars (K and M spectral classes) in the solar neighborhood, of which we have obtained deep images (down to a limit of about 19 magnitudes in the *I*-band filter at 880 nm) with narrow-band filters (11) centered at 740 and 914 nm (with a bandwidth of 10 nm). The survey is being conducted at the

0.8-m telescope of the Instituto de Astrofísica de Canarias (IAC80) at the Teide Observatory (OT) on Tenerife with a 1024 pixel by 1024 pixel charge-coupled device (CCD). One pixel of this detector projects 0.432 arc sec on the sky. The two narrow filters allow effective discrimination of faint red objects at separations larger than three to four times the full width at half maximum of the point source response, which was on average close to 1.5 arc sec for the first 52 targets of the program. Here we report on the discovery of a very red companion to the high-proper-motion M-class dwarf star G 196-3. The observations were performed on 25 January 1998. A comparison of the images taken at different wavelengths showed that a faint red companion was present at 16.2 arc sec southwest of the star (position angle = 210°; see Fig. 1). We have named this companion G 196-3B. Further optical *R* (660 nm) and *I* broad-band photometry (Table 1) was obtained at the 1-m Optical Ground Station (OGS) telescope on 19 March 1998, whereas infrared *J*-band (1200 nm) and *K*-band (2200 nm) data (Table 1) were collected at the 1.5-m Carlos Sánchez Telescope (TCS) on 24 March 1998. Both telescopes are located at the OT.

Inspection of the second Palomar Observatory Sky Survey red plates (obtained from the Space Telescope Science Institute Digitized Sky Survey) provides a  $2\sigma$  detection of G 196-3B at the position expected for a proper motion (12) common with that of G 196-3. Images in the *I* band taken with the imager spectrograph (ALFOSC) at the 2.5-m Nordic Optical Telescope (NOT) at the Roque de los Muchachos Observatory (ORM) on 16 February 1998 (with a pixel size of 0.187 arc sec) and with HIRAC on 3 June 1998 (pixel size, 0.109 arc sec) confirm that the faint object has a proper motion ( $\mu_{\alpha\cos\delta} = -0.5 \pm 0.1$  arc sec year<sup>-1</sup>,  $\mu_{\delta} = -0.3 \pm 0.1$  arc sec

and an Evaluation of the IPCC IS92 Emission Scenarios, J. T. Houghton et al., Eds. (Cambridge Univ. Press, Cambridge, 1995).

5. U. Schumann, *Atmos. Environ.* **31**, 1723 (1997); U. Schumann, Ed., *Air Pollution Research Report 58*. Publication EUR 16978 EN (Office for Official Publication of the European Communities, Luxembourg, 1996); R. R. Friedl, Ed., *NASA Reference Publication 1400* (NASA, Greenbelt, MD, 1997); G. P. Brasseur et al., *Atmos. Environ.* **32**, 2329 (1998).
6. D. S. Lee et al., *Atmos. Environ.* **31**, 1735 (1997).
7. L. K. Emmons et al., *ibid.*, p. 1851.
8. R. R. Dickerson et al., *Science* **235**, 460 (1987).
9. K. E. Pickering et al., *J. Geophys. Res.* **95**, 14049 (1990); K. E. Pickering et al., *ibid.* **97**, 17985 (1992).
10. J. Lelieveld and P. J. Crutzen, *Science* **264**, 1759 (1994).
11. P. Dias-Lalcaca, D. Brunner, W. Imfeld, W. Moser, J. Staehelin, *Environ. Sci. Technol.*, **32**, 3228 (1998).
12. D. Brunner, thesis, ETH Zurich, Zurich, Switzerland (1998).
13. A simple photostationary state equilibrium results from the following reaction cycle:  $\text{NO} + \text{O}_3 \rightarrow \text{NO}_2 + \text{O}_2$  (1);  $\text{NO}_2 + \text{h}\nu \rightarrow \text{NO} + \text{O}$  (2);  $\text{O} + \text{O}_2 + \text{M} \rightarrow \text{O}_3 + \text{M}$  (3) and is given by
 
$$[\text{NO}_2] = \frac{k_1[\text{NO}][\text{O}_3]}{J_{\text{NO}_2}}$$
 where  $k_1$  is the rate constant of reaction (1) and  $J_{\text{NO}_2}$  is the rate of the photolysis of  $\text{NO}_2$  in reaction (2). The photolysis rate  $J_{\text{NO}_2}$  was calculated for clear-sky conditions only. The uncertainty in the calculation of  $\text{NO}_2$  adds to the uncertainty in total  $\text{NO}_x$  by not more than 20%, because on average,  $\text{NO}_2$  was only a minor fraction (20 to 30%) of total  $\text{NO}_x$  at 9 to 12 km altitude. Nitrogen oxides values derived from measured  $\text{NO}_2$  concentrations were 33 pptv higher, on average, than those calculated from photostationary state  $\text{NO}_2$  (11). Given the  $\text{NO}_x$  concentration averaged over all measurements between December 1995 to May 1996 of 172 pptv, this represents a difference of about 20%.
14. ECMWF (European Centre for Medium-Range Weather Forecast) model at T213/L31 resolution—that is, with 31 vertical layers and 0.75° by 0.75° horizontal resolution.
15. H. Schlager et al., *J. Geophys. Res.* **102**, 10739 (1997).
16. D. D. Parrish et al., *ibid.* **98**, 2927 (1993).
17. C. Price, J. Penner, M. Prather, *ibid.* **102**, 5929 (1997); H. Levy II, W. J. Moxim, P. S. Kasibhatla, *ibid.* **101**, 22911 (1996).
18. W. T. Luke, R. R. Dickerson, W. F. Ryan, K. E. Pickering, L. J. Nunnermaker, *ibid.* **97**, 20647 (1992).
19. S. B. Smyth et al., *ibid.* **101**, 24165 (1996).
20. We define a large-scale plume as the sequence of at least four 2-min integrated  $\text{NO}_x$  samples that show an average increase relative to the background of at least 0.1 ppbv. The background level during a plume event was simply obtained by linear interpolation between the concentrations adjacent to the plume (Fig. 1). Given the (true air) speed of the aircraft of 250 m/s, four samples correspond to a flight leg of 120 km. A difference of 0.1 ppbv is well above the noise of the measurement (11) and represents a significant increase above background levels of typically 70 to 200 pptv (Table 1).
21. Using a higher PV value of 4 PVU for the tropopause definition, the fraction of samples obtained within plumes is 10.4% and 1.6% for the tropospheric and stratospheric samples, respectively. Thus, the probability to observe a large-scale plume rapidly decreases in the stratosphere.
22. F. Flatøy and Ø. Hov, *J. Geophys. Res.* **102**, 21373 (1997).
23. The NOXAR project was funded by the Swiss Federal Civil Aviation Authority (BAZL). We thank Swissair for the generous support and ECO Physics Inc. for the design of the instrumentation and the assistance during the measurements. We also acknowledge H. Wernli and M. Bourqui for the trajectory calculations and R. Luethi for providing data from his archive of satellite images, which were both of great help for the interpretation of the measurements.

20 July 1998; accepted 14 October 1998

Instituto de Astrofísica de Canarias, E-38200 La Laguna, Tenerife, Canary Islands, Spain.

\*To whom correspondence should be addressed. E-mail: rrl@lliac.es

REPORTS

year<sup>-1</sup>) consistent with that of the M-class star within 2σ error bars (13).

A low-resolution optical spectrum of G 196-3B (Fig. 2, top panel) was obtained at the NOT on 16 February 1998, using the low-resolution ALFOSC spectrograph, grating number 4 (dispersion, 3.2 Å per pixel; effective resolution, 16 Å), and a 2048 pixel by 2048 pixel detector. It shows distinctive features that are characteristic of temperatures lower than 2000 K. G 196-3B's spectrum is dominated by two pronounced absorptions centered on 769 and 868 nm. Both features have recently been identified as being due to a considerable broadening of the 766.4, 769.8 nm K I resonance doublet (14–16) and to molecular absorptions of CrH (17) at 861.1 and 869.6 nm and of FeH (17) at 869.2 nm, respectively. TiO and VO molecular absorptions, which are intense in spectra derived from M-type dwarfs, appear weak or nonexistent in our spectrum, possibly indicating the photospheric depletion of Ti and V atoms to form dust grains. All this, together with the comparison of our data with the spectra of similar resolution obtained for Kelu 1 (18) and DENIS objects (19), suggests that G 196-3B deserves to be considered as an appropriate candidate for the so-called L-type class (14). There is no evidence for emission of the hydrogen line H $\alpha$  (656.3 nm), and the atomic lines of Na I, Rb I, and Cs I, which are observed in other L-type objects, show up weakly in G 196-3B. Their weakness can be interpreted as an indication of low surface gravity, consistent with what would be expected of a very young object undergoing gravitational contraction. From the similarity of our spectrum to that of Kelu 1, we infer an effective temperature of 1800 ± 200 K for G 196-3B. The probability of finding a free-floating L-type field object in our survey (0.74 deg<sup>2</sup>) is rather small (≤4%) given the statistics of detections of similar objects achieved by the

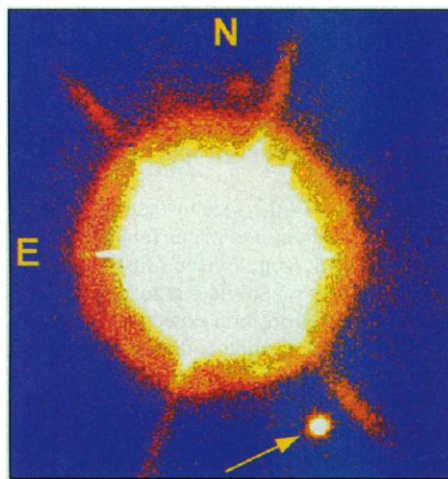


Fig. 1. I-band image taken at the NOT (36 × 36 arc sec<sup>2</sup>) showing the substellar companion G 196-3B, discovered at 16.2 arc sec SW (position angle = 210°) of the young nearby red star G 196-3.

large-scale infrared surveys Deep Near Infrared Survey (DENIS) (19) and Two-micron Massachusetts Sky Survey (2MASS) (20). This provides additional support for G 196-3B being a genuine companion to the M-class primary star.

A low-resolution optical spectrum of G 196-3 covering a wavelength range of 449 to 900 nm was obtained at the NOT with the same instrumental setup and on the same date as that of the companion. Using spectral indicators (21, 22) based on the strength of several TiO bands present in this wavelength interval, we classify our star as an M2.5 dwarf with an uncertainty of half a subclass. Broad-band *VRJHK* photometry (Table 1) obtained with the IAC80 telescope on 27 February 1998 and with the TCS telescope on 17 to 20 June 1998 is in agreement with this spectral classification. The optical spectrum is similar to that of M2-M3 dwarfs in young stellar clusters of solar metallicity. The observed optical and infrared colors present no strange anomaly that might be attributed to an unresolved less massive companion to G 196-3, and no indication of changes in the radial velocity is found beyond the uncertainties of our measurements (±6 km s<sup>-1</sup>), determined with high-resolution spectra taken at the Isaac Newton Telescope over a time interval of several hours to days. This makes it very unlikely that the star is actually a close-contact binary. The spectral type combined with the observed fluxes indicate that the star is at a minimum distance of 15.4 pc from Earth; this distance would correspond to the star's being at the hydrogen-burning stage on

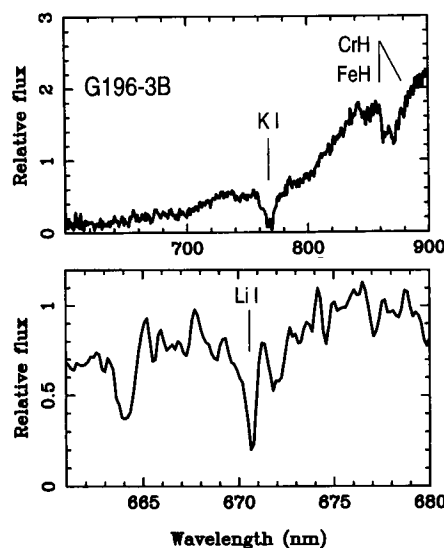


Fig. 2. (Top) Optical low-resolution spectrum of the substellar companion G 196-3B obtained at the NOT. The spectrum (normalized to unity at 813 nm) shows distinctive features of very low temperatures ( $T_{\text{eff}} \leq 2000$  K). (Bottom) Intermediate-resolution spectrum obtained at the WHT telescope showing the Li detection at 670.8 nm in G 196-3B.

the main sequence. As we discuss below, there are reasons to believe that the star is young and in a pre-main sequence phase; it is therefore at a more luminous evolutionary stage and consequently at a greater distance.

H $\alpha$  and H $\beta$  are seen in emission with equivalent widths (EWs) of 0.40 ± 0.03 nm and 0.33 ± 0.03 nm, respectively, indicating substantial chromospheric activity in G 196-3; this is also supported by the strong emission of Ca II H and K (EWs of 1.7 and 1.0 ± 0.1 nm, respectively) and other Balmer lines (23) (see Fig. 3), as well as by the star's being an extreme ultraviolet source (24). This when taken together with the high x-ray flux (48 × 10<sup>-13</sup> erg cm<sup>-2</sup> s<sup>-1</sup>) measured by the ROSAT All Sky Survey (RASS), which at the minimum distance of the star results in an x-ray luminosity of  $L_x = 1.36 \times 10^{29}$  erg s<sup>-1</sup>, supports the hypothesis that we are dealing with a young star. G 196-3 shows the same chromospheric and coronal properties of stars of similar temperatures in the young open cluster  $\alpha$  Persei [60 million years (My) old] (25) and slightly more activity than the average of its counterparts in the Pleiades (120 My) (26). The coronal and chromospheric properties, when examined in the light of the available data on the activity of stars of similar spectral type in these clusters (9, 10), suggest an age for G 196-3 of ~100 My; that is, intermediate between that of the  $\alpha$  Persei and Pleiades clusters.

An upper limit to the age of G 196-3 can be imposed from comparison to the Hyades cluster (600 My), where the average chromospheric and coronal emission of M2-M3 stars is considerably lower than in G 196-3. This star appears to be substantially younger than the Hyades, and hence we adopt 300 My, an age

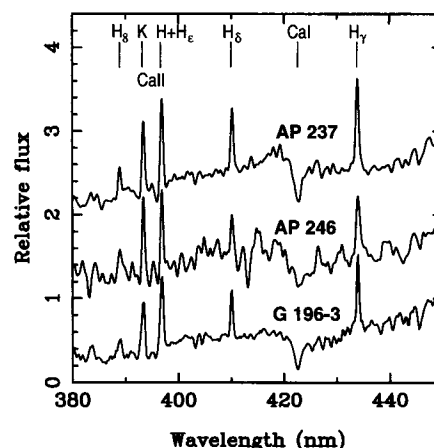


Fig. 3. Low-resolution spectra of the M2.5 type star G 196-3 (23) showing Ca II H and K and some Balmer lines in emission in comparison to other young stars of similar spectral type (AP246 is M3 and AP237 is M4) in the  $\alpha$  Persei cluster. Spectra have been normalized to unity at 450 nm, and a constant offset of 1 in the flux axis has been added for clarity.

intermediate between that of the Pleiades and Hyades, as a reasonable upper age limit. The lower age limit can be derived from observations of Li I at 670.8 nm. Lithium is a fragile element that burns efficiently in the interiors of fully convective stars over short time scales (a few tens of millions of years). Convection drains material from the stellar atmosphere into the innermost layers, where the temperature is high enough for Li burning to take place. There are several models (5, 6) in the literature that predict the Li depletion rate as function of mass for low-mass stars and give consistent results. A search was made for the Li I line in G 196-3, and an optical spectrum was obtained on 13 February 1998 with the Intermediate Dispersion Spectrograph with the 235-mm camera and a 1024 pixel by 1024 pixel CCD on the INT at the ORM. The H1800V grating gave a nominal dispersion of 0.053 nm per pixel and an effective resolution of 0.1 nm. The spectral range covered was 640 to 696.5 nm. We imposed an upper limit on the EW of 0.005 nm, which gives a Li depletion factor larger than 1000 with respect to its original abundance. This constrains the age of the star to be older than 20 My (27). All these considerations provide a most likely age for G 196-3 that locates our star in the pre-main sequence evolutionary phase and thus at a more luminous stage than expected for its main-sequence lifetime. According to the age range derived, the most probable distance from Earth to the system is  $21 \pm 6$  pc, the minimum value corresponding to the case of the primary star already on the main sequence and the maximum distance taking into account the youngest possible age.

Assuming this distance interval, we can estimate the luminosity ( $L$ ) of the companion G 196-3B from the measured  $I$  and  $K$  magnitudes and the  $K$  bolometric correction (28) as a function of the color ( $I$  through  $K$ ). The values obtained are  $\log L/L_{\odot} = -4.1$  when the oldest age (main sequence) is assumed and  $\log L/L_{\odot} = -3.6$  for the youngest age ( $L_{\odot}$  luminosity of the sun). The comparison

**Table 1.** Data for the G 196-3 system. Subscript c indicates the Cousins photometric system; UKIRT, photometric system of the United Kingdom Infrared Telescope; SpT, spectral type;  $M_{\odot}$ , mass of the sun.

Magnitudes and parameters	G 196-3	G 196-3B
$V_c$	$11.75 \pm 0.01$	
$R_c$	$10.67 \pm 0.01$	$20.78 \pm 0.10$
$I_c$	$9.41 \pm 0.01$	$18.28 \pm 0.05$
$J_{UKIRT}$	$8.12 \pm 0.02$	$14.73 \pm 0.05$
$H_{UKIRT}$	$7.47 \pm 0.02$	
$K_{UKIRT}$	$7.29 \pm 0.02$	$12.49 \pm 0.10$
SpT	$M2.5 \pm 0.5$	L class
$T_{\text{eff}}$ (K)	$3400 \pm 100$	$1800 \pm 200$
$\log L/L_{\odot}$	$-1.5 \pm 0.2$	$-3.8^{+0.2}_{-0.3}$
Mass	$0.40 \pm 0.05 M_{\odot}$	$25^{+15}_{-10} M_{\text{Jup}}$

of our optical and infrared magnitudes with the recent evolutionary tracks (29, 30), which include dust condensation, allows us to conclude that the mass of G 196-3B is  $25^{+15}_{-10}$  Jupiter masses ( $M_{\text{Jup}}$ ), where the upper and lower values result from the age limits discussed above.

An independent confirmation of the substellar nature of this faint companion was achieved with the detection of the Li I resonance doublet at 670.8 nm. We obtained an intermediate-resolution optical spectrum at the 4.2-m William Herschel Telescope (WHT) at the ORM on 6 April 1998 (Fig. 2, bottom panel) using the ISIS double-arm spectrograph with a grating of 316 grooves  $\text{mm}^{-1}$  and a 1024 pixel by 1024 pixel CCD, an instrumental setup that provided a nominal dispersion of 0.15 nm per pixel (an effective resolution of 0.3 nm). The EW of the doublet is  $0.5 \pm 0.1$  nm that, using model atmospheres (16), gives an atmospheric abundance consistent with no depletion at all of Li. The presence of Li, combined with the low atmospheric temperature, rules out the possibility that our object is a star. Any brown dwarf with a mass below  $65 M_{\text{Jup}}$  should preserve its initial Li content for its entire lifetime, and an object with such a small mass as that of G 196-3B should necessarily show a high Li content. Although in more massive substellar objects the presence of Li would help to determine its evolutionary stage more precisely through the time dependence of Li burning, for our object this detection provides a necessary check of consistency.

A more precise evolutionary status of G 196-3B can be determined with an accurate parallax measurement or the detection of deuterium in the atmosphere (or both). Deuterium, a more fragile nuclear species than Li, is burned (5, 31) in substellar-mass objects with masses above 12 to  $15 M_{\text{Jup}}$ . The consumption of deuterium provides a substantial part of the total luminosity of brown dwarfs during the early phase that takes from 1 to 100 My, depending on its mass and age. G 196-3B has probably burned its deuterium, but it could have preserved a detectable amount if its mass were indeed close to  $15 M_{\text{Jup}}$ . Detection of deuterium features (deuterated molecules, hyperfine-transition isotopic splitting, and so on) could contribute to better determination of the mass and evolutionary status of G 196-3B.

The distance of the system implies a physical separation between the two components of more than 250 astronomical units (AU), being 350 AU at 21 pc. It could be even larger if the system were younger and therefore more distant from the sun. This large distance and the high mass ratio of 16:1 between the two components favor the fragmentation of a collapsing cloud as the most plausible explanation for the formation of the

system (32, 33). The possibility cannot be excluded, however, that the accretion of matter in a protoplanetary disc may produce an object more massive than  $15 M_{\text{Jup}}$  at such large distances. Accretion discs extending up to several hundred astronomical units are known to exist around several stars (34). Surveys similar to that conducted here will provide a statistically significant number of substellar-mass companions that can be used to test the proposed formation mechanisms and may well promote the development of new ideas, as occurred because of the recent findings of giant planets with highly eccentric orbits around solar-type stars (35, 36). Of the 52 stars we have examined so far, only G 196-3 has shown a substellar companion at distances larger than 60 AU, which is the minimum physical distance that we can explore given the characteristics of our survey. We may infer from this that the percentage of stars with substellar companions of about this mass at this or larger distances may be on the order of 2%. This is similar to the number of stars that show such companions at distances less than 5 AU, according to searches based on radial velocity measurements (35, 36).

**References and Notes**

1. T. Nakajima *et al.*, *Nature* **378**, 463 (1995).
2. B. R. Oppenheimer, S. R. Kulkarni, K. Matthews, T. Nakajima, *Science* **270**, 1478 (1995).
3. B. R. Oppenheimer, S. R. Kulkarni, K. Matthews, M. H. van Kerkwijk, *Astrophys. J.* **502**, 932 (1998).
4. A. B. Schultz *et al.*, *ibid.* **492**, L181 (1998).
5. F. D'Antona and I. Mazzitelli, *Astrophys. J. Suppl.* **90**, 467 (1994).
6. I. Baraffe, G. Chabrier, F. Allard, P. Hauschildt, *Astrophys. J.* **446**, L35 (1995).
7. A. Burrows *et al.*, *ibid.* **491**, 856 (1997).
8. X-ray emission from low-mass stars is associated with the magnetic activity resulting from the interplay between stellar rotation and surface convective motions. The stellar rotation is a decreasing function of age in these stars. Young low-mass stars typically show rapid rotation, which favors the generation of enhanced magnetic fields and the heating of the outermost stellar layers, producing the x-ray emission.
9. A. Hempelmann, J. H. M. M. Schmitt, M. Schultz, G. Rüdiger, K. Stepien, *Astron. Astrophys.* **294**, 515 (1995).
10. S. Randich, J. H. M. M. Schmitt, C. F. Prosser, J. R. Stauffer, *ibid.* **305**, 785 (1996).
11. E. L. Martín, R. Rebolo, M. R. Zapatero Osorio, *Astrophys. J.* **469**, 706 (1996).
12. Proper motion values:  $\mu_{\alpha \cos \delta} = -0.2 \pm 0.1$  arc sec year<sup>-1</sup>,  $\mu_{\delta} = -0.2 \pm 0.1$  arc sec year<sup>-1</sup>; H. L. Giclas, R. Burnham Jr., N. G. Thomas, *The G Numbered Stars* (Lowell Observatory at Flagstaff, AZ, 1971).
13. Additionally, high-resolution spectra of the primary star G 196-3 and the faint companion G 196-3B, obtained at the Keck 10-m telescope (Mauna Kea Observatory, HI) by E. L. Martín and G. Basri, show that the radial velocity of the two components does coincide within 2 km s<sup>-1</sup>.
14. E. L. Martín, G. Basri, X. Delfosse, T. Forveille, *Astron. Astrophys.* **327**, L29 (1997).
15. C. G. Tinney, X. Delfosse, T. Forveille, F. Allard, *ibid.*, in press.
16. Ya. Pavlenko, M. R. Zapatero Osorio, R. Rebolo, paper presented at the Very Low-Mass Stars and Brown Dwarfs in Stellar Clusters and Associations Euroconference, La Palma, Spain, 11 to 15 May 1998.
17. D. Kirkpatrick *et al.*, *Astrophys. J.*, in press.

18. M. R. Ruiz, S. K. Leggett, F. Allard, *ibid.* **491**, L107 (1997).
19. X. Delfosse *et al.*, *Astron. Astrophys.* **327**, L25 (1997).
20. C. Beichman *et al.*, paper presented at the Very Low-Mass Stars and Brown Dwarfs in Stellar Clusters and Associations Euroconference, La Palma, Spain, 11 to 15 May 1998.
21. C. F. Prosser, J. R. Stauffer, R. P. Kraft, *Astron. J.* **101**, 1361 (1991).
22. E. L. Martín, R. Rebolo, A. Magazzú, *Astrophys. J.* **436**, 262 (1994).
23. E. Polomski, S. Vennes, J. R. Thorstensen, M. Mathioudakis, E. E. Falco, *ibid.* **486**, 179 (1997).
24. M. Lampton *et al.*, *Astrophys. J. Suppl.* **108**, 545 (1997).
25. G. Basri and E. L. Martín, *Astrophys. J.*, in press.
26. E. L. Martín *et al.*, *ibid.* **499**, L61 (1998).
27. G. Chabrier, I. Baraffe, B. Plez, *ibid.* **459**, L91 (1996).
28. M. S. Bessell, F. Castell, B. Plez, *Astron. Astrophys.* **333**, 231 (1998).
29. A. Burrows *et al.*, *Asp. Conf. Ser.* **134**, 354 (1998).
30. I. Baraffe, G. Chabrier, F. Allard, P. H. Hauschildt, *Astron. Astrophys.*, **337**, 403 (1998).
31. D. Saumon *et al.*, *Astrophys. J.* **460**, 993 (1996).
32. P. Artymowicz, *Asp. Conf. Ser.* **134**, 152 (1998).
33. P. Bodenheimer, *ibid.*, p. 115.
34. F. Bruhweiler *et al.*, *Bull. Am. Astron. Soc.* **191**, 47.03 (1997).
35. M. Mayor and D. Queloz, *Nature* **378**, 355 (1995).
36. G. Marcy, *ibid.* **391**, 127 (1998).
37. We thank N. González Pérez for assistance with the infrared observations at the TCS, J. Casares and I.

Martínez-Pais for their assistance at the INT, I. Baraffe and the Lyon group for providing us with new evolutionary models for very low masses before publication, E. Polomski for sending the published spectrum of G 196-3 in digitalized format, and E. L. Martín and G. Basri for sharing data before publication. This paper is based on observations made with the IAC80; the European Space Agency's OGS and the TCS, operated by the Instituto de Astrofísica de Canarias (IAC) at the OT; and the NOT, the INT, and the WHT, operated on the island of La Palma by the Isaac Newton Group at the ORM of the IAC. Partial financial support was provided by the Spanish Dirección General de Enseñanza Superior, project no. PB95-1132-C02-01.

7 August 1998; accepted 8 October 1998

## Requirement for MAPK Activation for Normal Mitotic Progression in *Xenopus* Egg Extracts

Thomas M. Guadagno and James E. Ferrell Jr.\*

The p42 mitogen-activated protein kinase (MAPK) is required for progression through meiotic M phase in *Xenopus* oocytes. This report examines whether it also plays a role in normal mitotic progression. MAPK was transiently activated during mitosis in cycling *Xenopus* egg extracts after activation of the cyclin-dependent kinase Cdc2–cyclin B. Interference with MAPK activation by immunodepletion of its activator MEK, or by addition of the MEK inhibitor PD98059, caused precocious termination of mitosis and interfered with production of normal mitotic microtubules. Sustained activation of MAPK arrested extracts in mitosis in the absence of active Cdc2–cyclin B. These findings identify a role for MEK and MAPK in maintaining the mitotic state.

Mitosis is initiated by the activation of Cdc2–cyclin complexes. In *Xenopus* egg extracts, three mitotic Cdc2–cyclin complexes have been identified; they are activated and inactivated sequentially, beginning with Cdc2–cyclin A1, followed by Cdc2–cyclin B1, and finally Cdc2–cyclin B2 (1). The last of the three, Cdc2–cyclin B2, is inactivated just after nuclear envelope breakdown (NEBD) (1). Chromatin condensation and NEBD persist throughout the remainder of M phase in the absence of active Cdc2. This persistence could be the result of slow reversal of the effects of Cdc2, or these aspects of mitosis could be actively maintained by some regulatory protein other than Cdc2.

Several lines of evidence raise the possibility that p42 MAPK (also called ERK2) participates in mitosis. MAPK activation is required for *Xenopus* oocyte maturation, and the regulation of oocyte maturation and is similar to regulation of mitosis in many im-

portant respects (2). Moreover, in sea urchin embryos (3), mammalian cell lines (4), and cycling *Xenopus* egg extracts (Figs. 1C; 2C; and 3, A and C) (5, 6), MAPKs are activated during mitosis. Finally, MAPKs have been implicated in the spindle assembly checkpoint in extracts and in a *Xenopus* cell line (XTC-2) (5–7), and there is precedent for proteins involved in this checkpoint to be involved in establishing the timing of an unperturbed mitosis (8). However, depletion of p42 MAPK or inhibition of p42 MAPK activation has no effect on the activation or inactivation of Cdc2 in cycling *Xenopus* egg extracts, which suggests that p42 MAPK might be dispensable for mitotic entry and exit (5).

We examined the role of p42 MAPK in mitosis in cycling extracts, monitoring not only Cdc2 activation and inactivation but also the main morphological hallmarks of mitosis—nuclear envelope breakdown, chromatin condensation, and microtubule dynamics. We prevented mitotic activation of p42 MAPK in cycling extracts by one of two treatments that inhibit MEK, the protein kinase that phosphorylates and activates MAPK: addition of the MEK inhibitor PD98059 (9) or immu-

nodepletion of MEK (10). Both approaches blocked p42 MAPK activation (Fig. 1, A and C). We then tested whether Cdc2 activity cycled normally in the absence of MAPK activation. Activation and inactivation of Cdc2 was similar in control and in PD98059-treated extracts and in mock-depleted and MEK-depleted extracts (Fig. 1, B and D), in agreement with previous reports (5).

We also tested whether nuclear envelope breakdown and re-formation and chromatin condensation and decondensation were altered in the absence of MAPK activation (11). We added low concentrations of demembrated sperm (500 per microliter) (12) to MAPK-inhibited and control cycling extracts, allowed nuclei to form, and took portions at various times to assess chromatin condensation by 4',6-diamidino-2-phenylindole (DAPI) staining and NEBD by phase-contrast microscopy. Both the control and PD98059-treated extracts underwent chromatin condensation and nuclear envelope breakdown 50 min after cycling was initiated (Fig. 2, A and B). However, the extracts in which MEK was inhibited exited mitosis prematurely (Fig. 2, A and B). The chromatin had decondensed and nuclear envelopes reformed by 60 min in the PD98059-treated extract but not until 75 min in the control extract. Thus the duration of mitosis (taken here to be the interval between NEBD and re-formation) in the MEK-inhibited extract was less than half that in the control extract. Premature mitotic exit was also observed with MEK-depleted extracts but not with mock-depleted extracts (Fig. 2C), and adding purified recombinant MEK to the MEK-depleted extracts restored mitosis to a normal length (Fig. 2D). These results indicate that MEK activation is necessary to maintain the mitotic state for a normal period of time. Because p42 and p44 MAPK are the only known substrates of MEK, and only p42 is present in egg extracts, these findings implicate p42 MAPK in maintenance of the mitotic state.

When MAPK is artificially activated before Cdc2 is activated, it can inhibit cyclin degradation and hence prolong Cdc2 activa-

Department of Molecular Pharmacology, Stanford University School of Medicine, Stanford, CA 94305-5332, USA.

\*To whom correspondence should be addressed. E-mail: ferrell@cmgm.stanford.edu